



# Effects of the PV-Generator's Terminals Connection to Ground on Electromagnetic Transients Caused by Lightning in Utility Scale PV-Plants

Y. Méndez, I. Acosta, J. C. Rodríguez, J. Ramírez and  
J. Bermúdez

Energy Conversion and Transport Department  
Universidad Simón Bolívar (USB)  
Caracas, Venezuela  
yarumendez@usb.ve

M. Martínez

Engineering Department  
Universidad La Salle Bajío (ULSB)  
León, Mexico  
mml104861@udelasalle.edu.mx

**Abstract**—The connection to ground of the negative or positive terminal of photovoltaic (PV) generators is a common practice to mitigate the effects of the potential induced degradation (PID), which is attributed to chemical reactions (ion's exchange) between the materials that constitute the PV-module during operation.

Furthermore, the complex topology of a utility scale PV-plant, its dimensions and the stored energy in the central PV-inverter's DC-link open the hypothesis that overvoltages at the DC- and AC-side of the PV-plant may arise during transients caused by impulse currents.

The objective of this publication is to explore the effects of this practice on the operation of utility scale MW-class PV-plants during transients caused by lightning.

**Keywords**-PID, DC-Link, Lightning, Utility Scale Photovoltaic, Transient, EMTP

## I. INTRODUCTION

This publication discloses a transient study related to utility scale PV-plants and the effects of the connection to ground of one of the PV-generator's terminals (positive or negative), which is an established practice in the PV-Industry. This situation opens the hypothesis that this practice may have additional effects on the study of transients during lightning.

Previous studies of the effect of the lightning surges on PV-plant and/or connecting POS or NEG terminal of PV-generator to ground has been previous studies reported [1], [2] and [3].

The content of the publication is structured as follows: An introduction to the PID problematic and technical characteristics of a real PV-plant is made on this section; the chosen simulation models (including DC-side, the central PV-inverter, AC-side and distribution system) are disclosed in section II.

A validation process is presented on section III and finally, in section IV a study based on simulations of the effects of the

PV-generator's connection to ground in combination with the stored energy at the PV-inverter's DC-link on transferred overvoltages caused by lightning is disclosed [4], [5], [6] and [7].

Potential induced degradation (PID) of PV-modules is an erratic condition mostly attributed to the result of the chemical reactions (ion's exchange) caused by low intensity leakage currents within the components of PV-modules, such as, PV-cells, cover glass, back foil or back glass, so-called Ethylene Vinyl Acetate film (EVA) and sealing materials, during its normal operation, duty cycle and the electric field (Fig. 1) [1].

A direct consequence of PID is a reduction of the PV-generator's electric power output and consequently the energy yield of the PV-Plant [1] and [2].

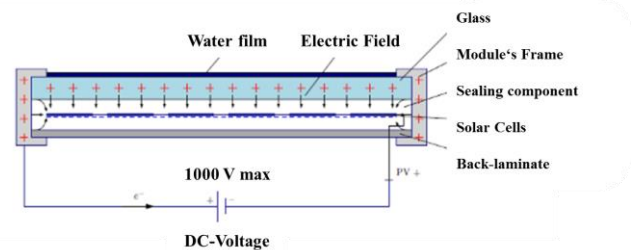


Figure 1. Schematic representation of PID (PV-module's side view). Ions exchange caused by the electric field during operation.

An established practice in the photovoltaic industry consists of connecting the positive (POS) or negative (NEG) terminal of the PV-generator to ground with the expectation that the potential distribution within the PV-module is further equalized and, consequently the effect of PID is reduced.

This practice may have other consequences, especially when transients arise in form of surges during lightning strikes, grid operation, energization, etc. at the AC- and DC-side of the PV-plant. This study was conducted during a research project on a real MW-Class PV-plant with the following components.

Fig. 2 depicts a schematic block diagram of the evaluated PV-plant and its general technical description are described as follows and in [6]:

- Thin-film frameless PV-modules, with 10 PV-modules per PV-string in order to reach the nominal voltage of at least 700 V<sub>DC</sub> for the required operation of the PV-inverters.
- 2 central PV-inverters (800 kW rated active power); 6 combiner boxes (GCBs) with 9,000 PV-modules connected to a PV-inverter and the remaining 6 GCBs or 9,200 PV-modules to the second PV-inverter.
- The max. DC short-circuit current is 1,098 A and 1,122 for each PV-inverter with a total of short-circuit current of 2,220 A for the whole PV-plant.
- Aluminum-based mounting (racking) system for the PV-modules with meshed grounding (earthing) system in order to minimize step- and touch-voltages with an additional grounded fence.

An impulse generator (10/350μs), which was installed within the PV-plant in order to evaluate surges and intentionally evaluate abnormal operation conditions.

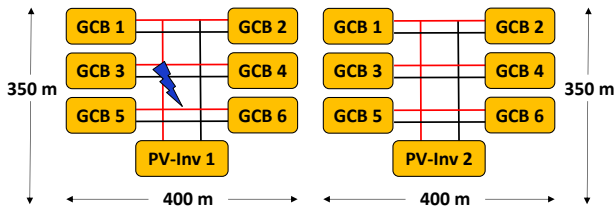


Figure 2. Utility scale PV-plant in block diagrams disclosing the short-circuit and surge current injection point close to the combiner box (GCB) 5.

## II. APPROACH AND MODELING

The components of the PV-plant were modeled in form of concentrated elements and PI-Diagrams calculated at a frequency of 250 kHz using the program EMTP-ATP. The models used are disclosed in the following subsections and in [6].

### A. PV-Modules/PV-Strings and PV-Tables

The PV-technology analyzed was frameless thin-film PV-modules, which is already in operation in the real PV-plant. Fig. 3 depicts the simulation model chosen for a PV-table formed by 5 PV-strings (with 10 PV-modules/PV-string, for a total of 50 PV-modules) in the frequency range from 150 kHz to 30 MHz.

A floating open-circuit DC-source  $V_{oc\_String}$  is connected in parallel with a diode in order to represent an approximate model of the  $V$ - $I$  Characteristic of the PV-string ( $PV_{Cells}$ ), as shown in Fig. 3 and Fig. 4.

The short-circuit temperature-dependent resistance  $R_{sc}$  with a value of 4.00 Ohm/GCB accounts for the limitation of the

prospective short circuit current  $I_{sc}$ , expected for every GCB of approx. 160.00 Amps (with rated total solar irradiance  $G_{PV}$  on the plane of the PV-generator of approx. 800.00 W/m<sup>2</sup> at ambient temperature).

The PV-string capacitance  $C_{PV}$  of the solar cells accounts for the space charge capacitance  $C_{sc}$ , the transition carrier capacitance  $C_{ic}$  and the diffusion capacitance  $C_D$ , which are intrinsic to the semiconductor material; for this frequency range a value of 18.00 nF for a PV-string and 3.20 μF for a GCB was chosen [7].

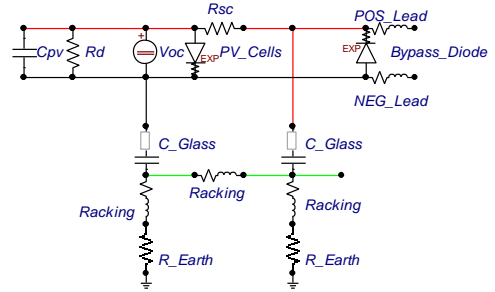


Figure 3. Model of one PV-string (10 PV-modules) with mounting (racking) system and grounding resistances.

A shunt diffusion resistance ( $R_d$ ) of the semiconductor material with a value of 464.00 Ohm for a PV-string and 2.90 Ohm for the GCB is assumed; these elements may introduce additional high frequency oscillation damping (observed in the experiments at the real PV-plant).

The capacitance of the PV-modules' glass-foil  $C_{Glass}$  with a value of 6.20 nF of the PV-modules is considered, in order to reflect the floating condition of the solar cells with respect to the racking system and ground [8].

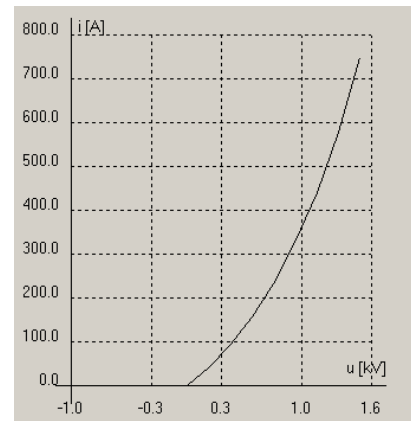


Figure 4.  $V$ - $I$  characteristic for the diode modeling the PV-string (10 PV-modules connected in series).

The mounting (racking) system is represented by resistances  $R_{Rack}$  and inductivities  $L_{Rack}$  with values of 1.00 mOhm and 3.00 μH respectively;  $R_{Earth}$  is the grounding resistance with a value of 10.00 Ohm corresponding to a low resistivity soil (< 200.00 Ohmm). Fig. 5 shows a representation of 8 PV-tables (400.00 PV-modules or a quarter of a combiner box or GCB).

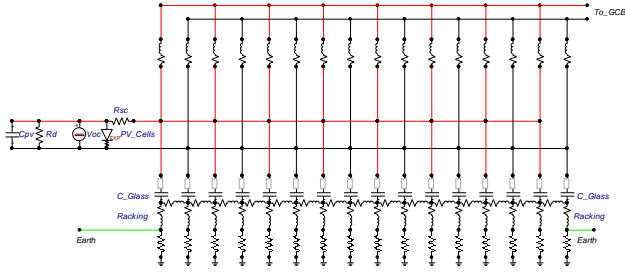


Figure 5. Simulation model of 8 PV-tables including the (a quarter of a GCB, 40 strings or 400 PV-modules), mounting (racking) system and grounding resistances

A more detailed model of the PV combiner box (GCB) is showed on Fig. 6, where the disconnection switch and the overvoltage protection (OVP) are depicted. The OVP is modeled by a non-linear element and a capacitance connected in parallel with value of 6.50 nF per connection terminal; the curve of the OVP is showed on Fig. 7 and especially designed for DC applications up to a nominal voltage of 1000 V.

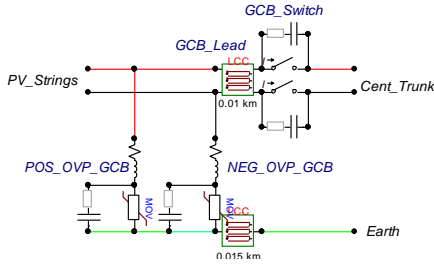


Figure 6. Model of the combiner boxes (GCB) with overvoltage protection (OVP) on the positive and negative terminals.

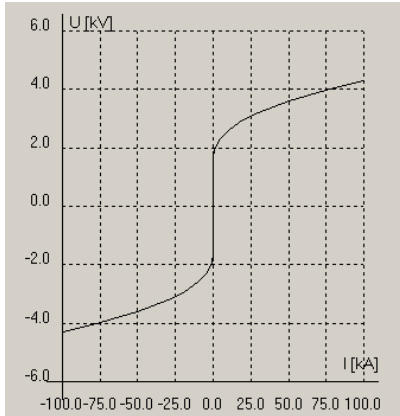


Figure 7. DC MOV's curve.

The model chosen for the cables connecting the PV-strings was a PI-equivalent calculated at a frequency of 250.00 kHz. The cables do have a cross-section of 50.00 mm<sup>2</sup> and are installed 2.20 m above the soil.

The cables (central trunk), connecting the GCBs to the PV-inverter, have a cross-section of 250.00 mm<sup>2</sup> and are buried 0.25 m under the soil.

The grounding cables were included and modeled.

The surge generator consists of a capacitor bank in series with an inductivity in order to generate the surge current for the experiments (10/350 μs, charge voltage up to 20kV), as showed in Fig. 8.

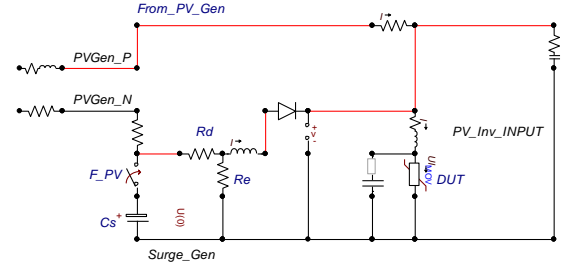


Figure 8. Model of the surge generator with OVP (Device under Test or DUT) connected between the POS and the NEG of the mains of the PV-inverter at the DC-side.

### B. MW-Class PV-Inverter (including DC-Link) and OVP

A model for the PV-inverter in form of surge impedances for fast transient studies was implemented (Fig. 9) [6].

At the DC-side, the following parameters of the PV-inverter (Maximum Power Point Tracker or MPPT) are considered:  $R_{dcs}$  (ohmic losses) and  $L_{dcs}$  (coils), which are characteristic for connections and terminals on the converter's DC side (depicted at the left hand side of Fig. 9).

The DC-link capacitance  $C_{DC\_Link}$  was modeled as a concentrated value. At the PV-inverter's AC-Side, the model neglects the mutual capacitance between phases and considers mainly the  $R_{gs}$  (ohmic losses) and  $L_{gs}$  (coils), which are characteristic for connections and terminals on the converter's AC side (including the harmonic filters).

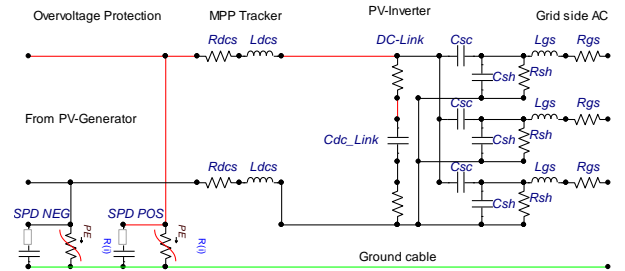


Figure 9. PV-Inverter (Converter) model used for transient studies including DC- and AC-Side in floating Y-connection).

A concentrated impedance in form of a shunt resistance  $R_{sh}$  and shunt capacitances to ground  $C_{sh}$  of the circuit represents the commercial optical or low voltage circuit electronic control boards and corresponding power electronics' drive circuits.

The parameter  $C_{sc}$  accounts for the intrinsic capacitance of the semiconductor material, such as IGBTs and gel-based isolating material (see Table I).

### C. Low and Medium AC Voltage Cables

The non-shielded low voltage (LV) cables connecting the PV-inverter to the low voltage side of the distribution

transformer were modeled with a PI-equivalent model, one per phase and one additional copper conductor for grounding.

Similarly, the medium voltage (MV) cables with a sheath connecting the primary side of the distribution transformer to the MV grid were simulated and calculated with a PI-equivalent at 250 kHz (see Table II).

TABLE I. PV-INVERTER'S PARAMETERS

Parameter	Value	Units
$R_{dcs}$	0.1	Ohm
$L_{dcs}$	1.0	$\mu\text{H}$
$R_{sh}$	250.0	Ohm
$C_{sh}$	0.1	nF
$C_{sc}$	1.0	nF
$C_{DC\_Link}$	2400.0	$\mu\text{F}$
$L_{gs}$	3.0	mH
$R_{gs}$	0.1	Ohm

TABLE II. LV AND MV CABLES PARAMETERS.

Section	Radius [mm]	Length [m]	$\epsilon$ [-]	$\rho$ [Ohmm]
LV	17.90	150.00	2.40	10.60E-5
LV <sub>Earth</sub>	8.95	150.00	2.20	10.60E-5
MV	34.50	300.00	2.70	10.60E-5
MV <sub>Earth</sub>	34.50	300.00	2.20	10.60E-5

#### D. AC Low (LV) and Medium (MV) Voltage (MV) MOVs

The model chosen for the LV and MV MOVs was in form of a nonlinear resistance with a capacitor connected in parallel per phase (see Table III, Fig. 10 and Fig. 11).

TABLE III. LV AND MV MOVs.

Section	$R_{MOV}$ [Ohm]	$L_{MOV}$ [ $\mu\text{H}$ ]	$C_{Parallel}$ [nF]
LV MOV	1.00E-4	0.50	6.50
MV MOV	1.00E-4	0.50	20.00

#### E. Distribution Transformer

The PV-plant is equipped with a distribution transformer, whereby the primary side is connected to the MV distribution network (20.00 kV) and the secondary side (0.40 kV) to the PV-Inverter's LV network (see Table IV). The transformer was modeled as a BCTRAN element without saturation.

TABLE IV. TRANSFORMER MODELING (COUPLING CAPACITANCES).

Voltage	$C_{Shunt}$ [nF]	$C_{Coupling}$ [nF]
20.00 kV (Star)	0.50	0.25
0.40 kV (Star)	0.10	0.25

The grounding systems of the PV-plant, fences and transformer were galvanic connected to each other and firmly grounded.

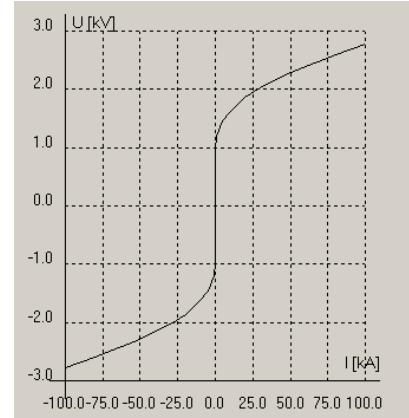


Figure 10. LV MOV's curve.

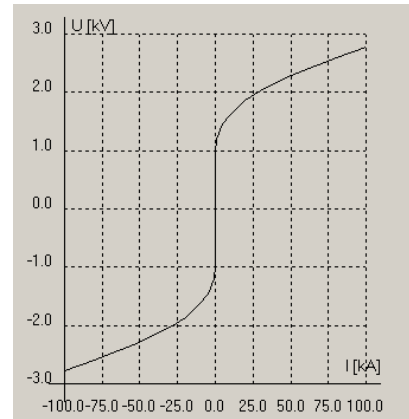


Figure 11. MV MOV's curve.

### III. SIMULATION VALIDATION

#### A. PV Transient Response against Surges

In order to validate the models and evaluate an additional operation condition at the overvoltage protection system (OVP) in terms of transient current and voltages, a surge current of 2.00 kA (10/350  $\mu\text{s}$ ) was imposed on the PV-Inverter's connection box at the DC-side by means of an impulse generator in a previous research [6].

The OVP was connected between the POS and NEG terminals and the PV-photocurrent of the farthest combiner box (GCB 1) was superimposed during the surge event and added up to the surge current generated by the impulse generator as depicted in the plots. For validation purposes, the measured and simulated transient response of voltage and currents at the PV-plant is depicted in Fig. 12 and Fig. 13.

In terms of comparison, an acceptable agreement is observed in the measurement and simulation, although this agreement is only for the consideration of the surge condition. The high-frequency oscillation observed in the simulation is

mainly caused by the lossless approach of the modeling at 250 kHz.

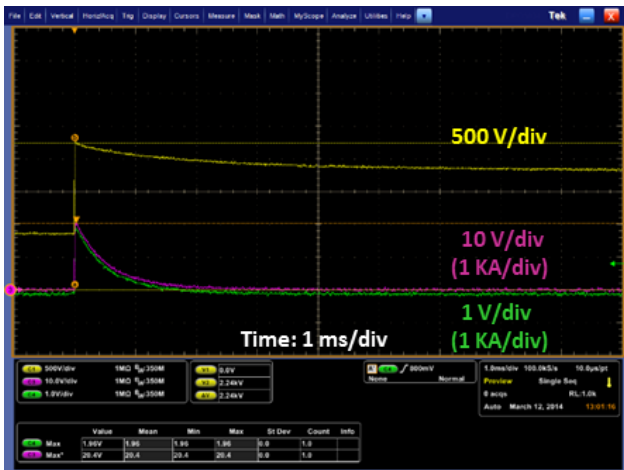


Figure 12. Measured impulse voltage (yellow line), impulse current through the surge generator (green) and total impulse current through the OVP (magenta) with the farthest GCB 1 connected (1,600 PV-modules/String, initial  $V_{oc}$  of approx. 845 Vdc).

At the initial phase from 0 to 250 ms of the simulated transient on Fig. 13, an exponential-type increase of the DC voltage is observed; this condition may be associated to the transient condition of the DC voltage, the steady state of the voltage is approx. 845 V, which is the open circuit voltage of the PV-generator at steady state.

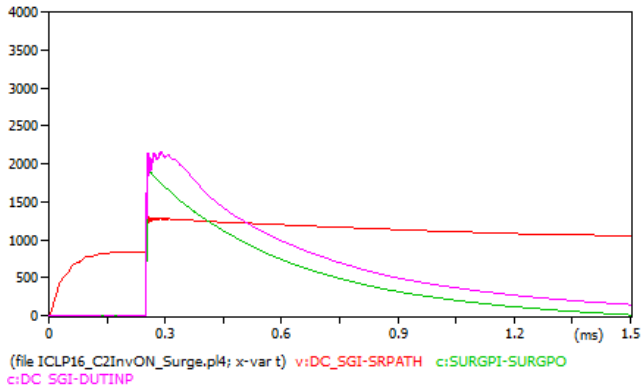


Figure 13. Simulated impulse voltage (red line), impulse current through the surge generator (green) and total impulse current through the OVP (magenta) with the farthest GCB 1 connected (1,600 PV-modules @ 10 PV-modules/String, initial  $V_{oc}$  of approx. 845 Vdc).

#### IV. EFFECT OF THE PV-GENERATOR'S TERMINAL CONNECTION TO GROUND AND THE STORED ENERGY ON THE DC-LINK ON THE TRANSIENT RESPONSE DURING LIGHTNING

In order to explore the effects of the PV-generators' terminal connection to ground in combination with the DC-link's stored energy ( $C_{DC\_Link}$  on Fig. 9 and Table I) on the transient response, a simulation study was conducted with the program ATP-EMTP [9]. The following parameters were considered in the simulation:

- Lightning current or surge condition in form of a transient Heidler current source 50 kA (10/350  $\mu$ s), injected into the racking system of combiner box 5 or GCB 5 at PV-plant's DC-side (see Fig. 2)
- Initial PV- $V_{oc}$  and DC-link voltage: 1000 V, which represents the max. DC voltage in most of PV installations [5].
- The DC- and AC-side of the PV-plant, such as the combiner boxes (GCBs) and the PV-inverter's on Fig. 2, are equipped with varistor-based surge protection devices (SPDs curve depicted in Fig. 7).
- The distribution transformer's low voltage side is not protected with SPDs.
- A group of 6 combiner boxes is connected to one PV-inverter and simulated.
- The chosen time-step of the simulation was 0.05  $\mu$ s for a total simulation time of 5.00 ms.

#### A. Simulations Results: AC-Side of the Central PV-Inverter and Distribution System

The transferred overvoltages from the DC to AC side at the power transformer's LV side and PV-inverter's AC side, when the PV-generator's POS or NEG is connected to ground, are depicted in Fig. 14 to Fig. 17 respectively, taking in consideration that the surge current is injected at the DC-side.

Concerning the distribution transformer an increase in the transient voltage is observed, when the lightning current is injected after 250 ms at the DC-side of the PV-plant (Fig. 14 and 15); as a result an overvoltage is transferred from the DC- to AC-side of the installation. The magnitude of the overvoltage is not harming the transformer (independent of the POS or NEG grounding).

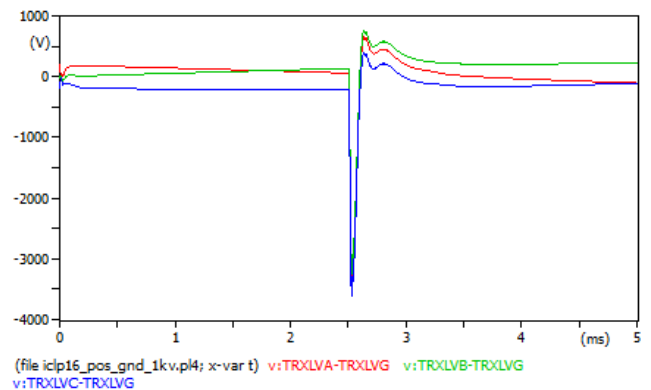


Figure 14. Distribution power transformer's LV-side: transient phase AC voltage with a surge after 250 ms, when the PV-generator's POS is grounded.

In regards to the AC-side of the PV-inverter an increase in the voltage magnitude is observed, when the lightning current is injected after 250 ms at the DC-side of the PV-plant (Fig. 16 and 17); as a result an overvoltage is transferred from the DC- to the AC-side of the PV-inverter and probably over the grounding system. The magnitude of the overvoltage is not

harming the PV-inverter (independent of the POS or NEG grounding), although remarkable differences in the transient form are depicted (in terms of waveform and peak values).

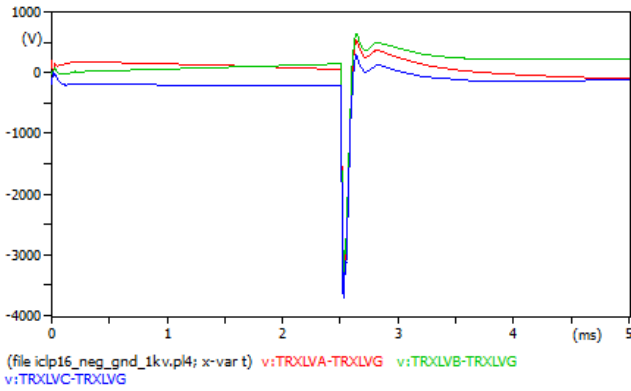


Figure 15. Distribution power transformer’s LV-side: transient phase AC voltage with a surge after 250 ms, when the PV-generator’s NEG is grounded.

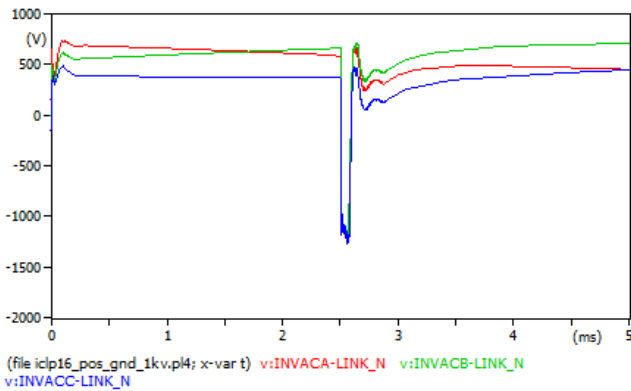


Figure 16. PV-inverter’s AC-side: transient phase AC voltage with a surge after 250 ms, when the PV-generator’s POS is grounded.

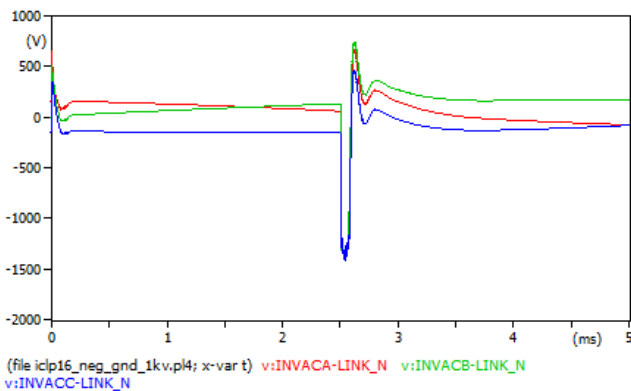


Figure 17. PV-inverter’s AC-side: transient phase AC voltage with a surge after 250 ms, when the PV-generator’s NEG is grounded.

Considering the impulse current of 50 kA injected on the DC-side at the GCB 5 (Fig. 2), the magnitude of the transferred overvoltages do not harm the transformer nor the PV-inverter’s DC-side; provided that a properly designed grounding system

and the overvoltage protection system (OVP) are well designed and installed at both sides of the PV-plant.

### B. Simulations Results: DC-Side of the PV-Plant

The transient induced overvoltages at the PV-plant’s DC-side, when the PV-generator’s POS or NEG is connected to ground, are depicted in Fig. 18 to Fig. 21.

The OVP-device connected to the grounded PV-generator’s terminal is exposed to lower overvoltages and shall dissipate less energy during the transient condition.

The transient condition and voltage distribution is not symmetrical between the POS and NEG, when one of the terminals are connected to ground and this may have influence in the duty cycle of the OVP system.

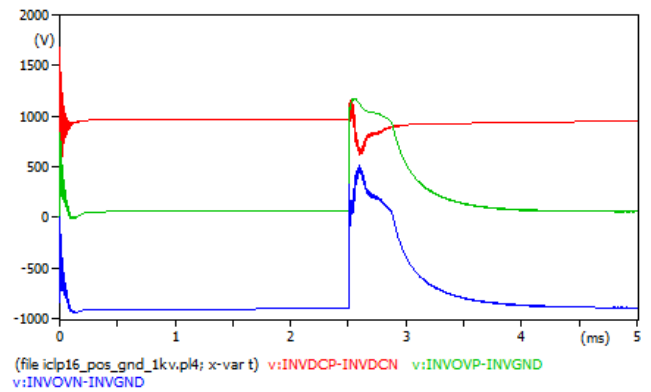


Figure 18. PV-inverter’s DC-side: transient voltage plots with a surge after 250 ms, when the PV-generator’s POS is grounded (POS-NEG: red, POS-Ground: green and NEG-Ground: blue).

A similar situation is observed with the combiner box 5 affected by lightning (GCB 5) and depicted in Fig. 20 and Fig. 21. Independently of the terminal grounding, the induced overvoltage between POS and NEG is not harming the electrical installation, due to the operation of the OVP. On the other side, the potential difference between POS-NEG and NEG-Ground is higher for the case with the PV-generator’s POS terminal connected to ground, as depicted in Fig. 19.

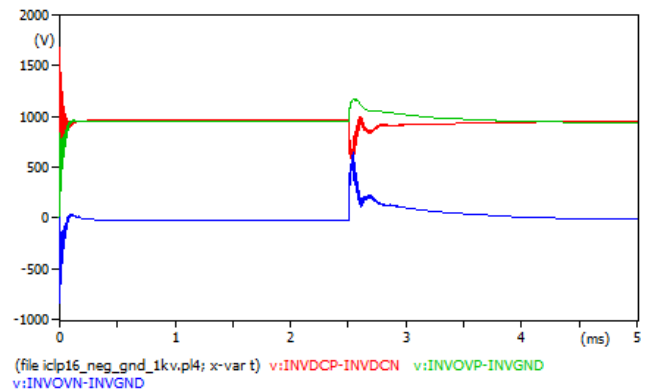


Figure 19. PV-inverter’s DC-side: transient voltage plots with a surge after 250 ms, when the PV-generator’s NEG is grounded (POS-NEG: red, POS-Ground: green and NEG-Ground: blue).

The effect of the PV-generator's terminal connection to ground references the chosen terminal's voltage to zero-potential level, indeed an offset of the grounded PV-generator's terminal to ground is observed.

The OVP-device connected to the grounded PV-generator's terminal is exposed to lower overvoltages and shall dissipate less energy during the transient condition. The transient condition and voltage distribution is not symmetrical between the POS and NEG, when one of the PV-Generator's terminals are connected to ground (Fig. 20 and 21).

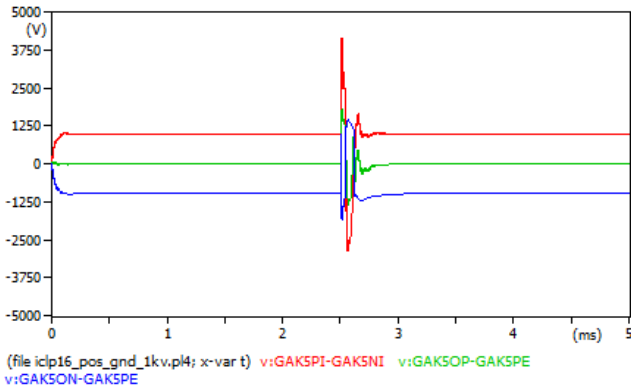


Figure 20. PV-generator's combiner box 5 (struck by lightning): transient voltage plots with a surge after 250 ms, when the PV-generator's POS is grounded (POS-NEG: red, POS-Ground: green and NEG-Ground: blue).

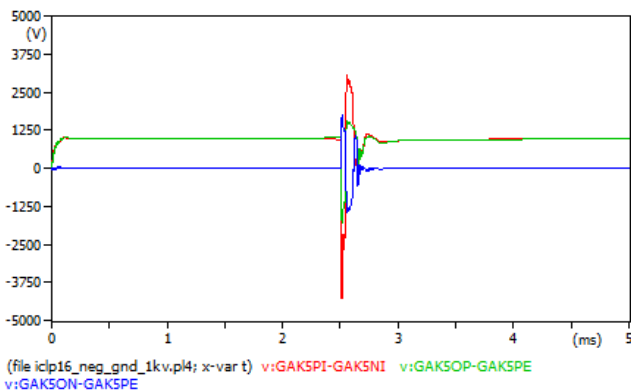


Figure 21. PV-generator's combiner box 5 (struck by lightning): transient voltage plots with a surge after 250 ms, when the PV-generator's NEG is grounded (POS-NEG: red, POS-Ground: green and NEG-Ground: blue).

### C. Simulations Results: Energy Stored on the DC-Link of the PV-Inverter and its effect on transient voltages

The transient overvoltage and current simulated at the PV-inverter's DC-link, when the PV-generator's POS or NEG is connected to ground, are depicted in Fig. 22 and Fig. 23.

Considering the 50 kA impulse current is injected on the vicinity of the combiner box (GCB 5) and the fact that the OVP-devices are biased during the surge, a portion of the energy stored in the PV-inverter's DC-link in form of transient current may flow through the OVP-devices. This situation

should be considered in the dimensioning of the lightning protection and OVP system.

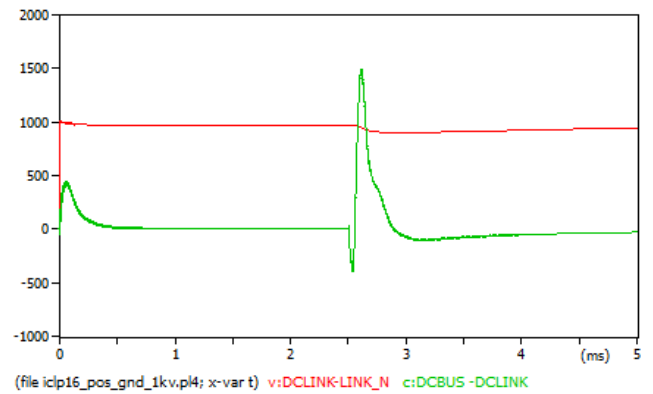


Figure 22. PV-inverter's DC-link: transient voltage and current plot with a surge after 250  $\mu$ s, when the PV-generator's POS is grounded (DC-Link voltage: red and DC-Link current: green).

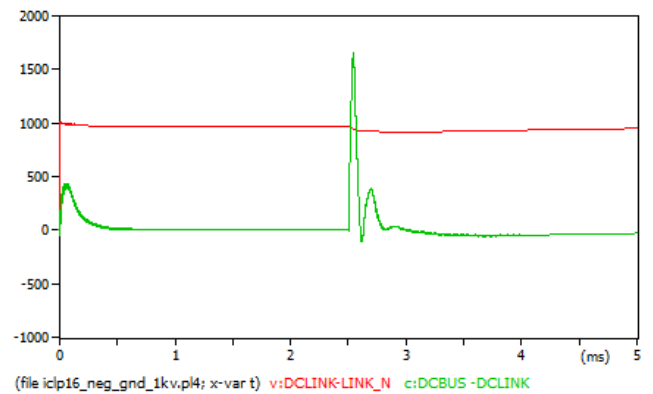


Figure 23. PV-inverter's DC-link: transient voltage and current plot with a surge after 250  $\mu$ s, when the PV-generator's NEG is grounded (DC-Link voltage: red and DC-Link current: green).

Fig. 24 and 25 depict the dissipated energy during the transient condition by the OVP devices (SPDs) connected at the PV-inverter's DC-side, which are stressed additionally.

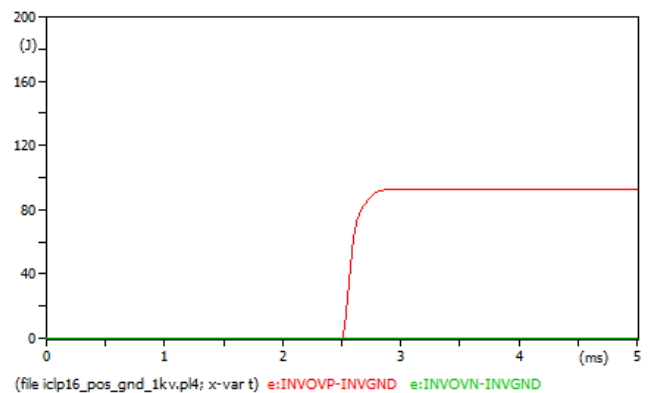


Figure 24. PV-inverter's DC-OVP: dissipated energy by the OVP plot with a surge after 250  $\mu$ s, when the PV-generator's POS is grounded (OVP-POS: red and OVP-NEG: green).

Although the injected transient lightning current's peak value is 50 kA, a value of 100 J, when the POS terminal is grounded, and 160 J, when the NEG terminal is grounded, are observed. The grounding of the NEC terminal leads to an increased energy dissipation at the OVP system connected at this terminal.

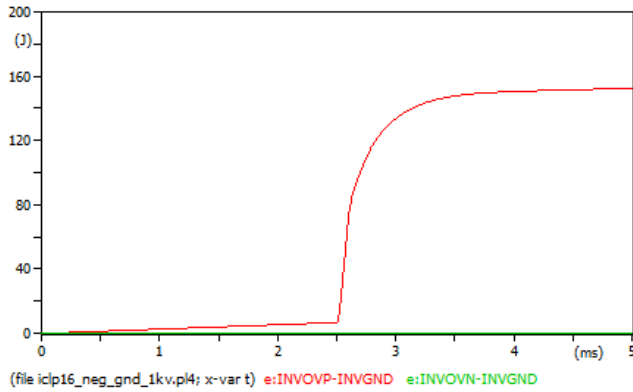


Figure 25. PV-inverter's DC-OVP: dissipated energy by the OVP plot with a surge after 250  $\mu$ s, when the PV-generator's NEG is grounded (OVP-POS: red and OVP-NEG: green).

## V. CONCLUSIONS

The connection to ground of the PV-generator's positive or negative terminal for PID mitigation has additional consequences on the dynamic response of the PV-plant during transients.

Although a low amplitude surge of 50 kA peak was simulated, additional stress on the installation is added by the energy stored at the DC-link's capacitor.

The transient response and voltage distribution are asymmetrical (offset condition) with respect to ground between the POS and NEG, when one of the PV-generator's terminals is connected to ground.

When the NEG of the PV-installation is connected to ground, the OVP system is additionally stressed from an

energy dissipation point of view. The topology of the connection of SPDs (POS-NEG-ground, Y-connection or T-connection in PV-DC systems) plays an important role in the mitigation of overvoltage transient conditions during lightning in PV utility scale plants.

## ACKNOWLEDGMENT

The authors gratefully acknowledge the Universidad Simón Bolívar (USB), Universidad de la Salle Bajío (ULSB) and the Murayh Consultancy Company for the academic and financial support of this research work.

## REFERENCES

- [1] J. Bergohld, T. Weber, and S. Pingel, "PID und Korrelation mit Felderfahrungen", 31. Symposium Photovoltaische Solarenergie, Mar. 2012.
- [2] IEC TS 62804-1:2015: "Photovoltaic (PV) modules - Test methods for the detection of potential-induced degradation - Part 1: Crystalline silicon", IEC-International Electrotechnical Commission, Ed. 1.0 2015.
- [3] C. Charalambous, N. Kokkinos, N. Christofides, M. Z. A. Ab Kadir, C. Gomes, "A Simulation Tool to Assess the Lightning Induced Over-Voltages on DC Cables of Photovoltaic Installations". Proc. 30th International Conference on Lightning Protection - ICLP, Oct. 2010.
- [4] J. Birkl, P. Zahlmann, "Specific requirements on SPDs installed on the DC-side of PV-generators". Proc. 30th International Conference on Lightning Protection - ICLP, Oct. 2010.
- [5] IEC 61643-12: "Low-voltage surge protective devices - Part 12: Surge protective devices connected to low-voltage power distribution systems - Selection and application principles", IEC-International Electrotechnical Commission, Ed. 2.0 2008-11.
- [6] Y. Méndez, and O. Mayer, "Effekte des am PV-Generator geerdeten negativen Pols auf transiente Vorgänge in PV-Zentralwechselrichtern". 31. Symposium Photovoltaische Solarenergie, Mar. 2016.
- [7] S. Schattner, "Die elektromagnetische Verträglichkeit und der Blitzschutz von Photovoltaik-Anlagen", Ph.D. dissertation, Dept. Elect. Eng., Karlsruhe Institute of Technology (KIT), Sep. 2001.
- [8] J. Kirchhof, C. Bendel, P. Funtan and G. Klein, "Sicherheitsaspekte bei Einsatz und Prüfung von transformatorlosen Wechselrichtern - Ergebnisse aus dem Projekt SIDENA", 21. Symposium Photovoltaische Solarenergie, Germany, Mar. 2006.
- [9] A. Greenwood, "Electrical Transient in Power Systems - Second Edition," John Wiley & Sons, U.S.A., 1991.